Ceria Nanocrystals Supporting Pd for Formic Acid Electrocatalytic Oxidation: Prominent Polar Surface Metal Support Interactions

Lin Ye[a‡], A. Hanif Mahadi[a‡], Chalathan Saengruengrit[b], Jin Qu[a], Feng Xu[a], Simon M. Fairclough[a], Neil Young[c], Ping-Luen Ho[a], Junjun Shan[d], Luan Nguyen[d], Franklin F. Tao[d], Karaked Tedsree[b]* and S.C. Edman Tsang[a]**

[a] The Wolfson Catalysis Centre, Department of Chemistry, University of Oxford, Oxford, OX1 3QR, UK.

[b] Department of Chemistry, Faculty of Science, Burapha University, Bangsaen, Chonburi, 20131, Thailand.

[c] Department of Materials, University of Oxford, Oxford, OX1 3PH, UK.

[d] Department of Chemistry, University of Kansas 1501 Wakarusa Dr. Lawrence, KS 66047, USA.

ABSTRACT: Ceria has been widely used as support in electrocatalysis for its high degree of oxygen storage, fast oxygen mobility and reduction and oxidation properties at mild conditions. However, it is unclear what are the underlying principles and the nature of surface involved. By controlling the growth of various morphologies of ceria nanoparticles, it is demonstrated that the

cubic-form of ceria, predominantly covered with higher energy polar surface (100), as support for Pd gives much higher activity in the electrocatalytic oxidation of formic acid than ceria of other morphologies (rods and spheres) with low indexed facets ((110) and (111)). High resolution TEM confirms the alternating layer-to-layer of cations and anions in (100) surface, the electrostatic repulsion of oxygen anions within the same layers gives intrinsically higher oxygen vacancies on this redox active surface in order to reduce surface polarity. DFT calculations suggest that the properties of fast oxygen mobility to re-oxidize the CO-poisoned Pd may arise from the overdosed oxygens on these ceria surface layers during electro-oxidation hence sustaining higher activity.

Keywords: ceria; noble metal; electrocatalysis; facet; polarity

Cerium oxide (CeO_2) has been extensively studied as highly active redox catalyst or support in catalysis and electrocatalysis.[1] Its catalysis properties originates from its remarkable fast Ce^{4+}/Ce^{3+} redox cycle, high oxygen storage and fast surface oxygen mobility, etc.[2] According to literature, surface area, oxygen vacancy, size and morphology, and exposed crystal face are considered as important factors which influence the overall catalytic properties of ceria.[3] For example, CeO_2 nanoparticles display better catalytic activity due to increasing number of oxygen defects as the crystallite size decreases.[4] In addition, the exposed crystal faces which are dependent on the shapes of ceria can also play an important role.[1b, 3, 5] As a result, noble metal (NM) nanoparticle dispersed on ceria as catalysts are among the systems long known to exhibit strong metal-support interaction (SMSI) effects.[6] Formic acid (HCOOH) is an attractive portable liquid fuel with energy density per volume than compressed hydrogen gas to supply PEM fuel

cell applications.[7] Pd has been well-regarded as the most effective metal component in an efficient catalyst for electrocatalytic formic acid oxidation in liquid phase.[8] However, their activity and selectivity seem to depend significantly on support interactions and in some cases, metal can subject to rapid or mild CO poisoning. Many attempts have been made to boost the performance of Pd electro-catalysts. Wang and co-workers[9] reported that Pd-CeO_2/C shows more enhanced electrocatalytic activity and improved kinetics for formic acid oxidation than conventional Pd/C. They proposed that CeO_2 promotes the proceeding of the direct oxidation pathway (dehydrogenation) to CO_2/H_2 over the dehydration pathway to CO/H_2O. Zhao et al.[10] proposed that good activity toward anodic methanol oxidation over Pt–CeO_2/C catalyst can be obtained from oxygen vacancies in CeO_2 providing active sites to oxidize CO-like poisoning species adsorbed on Pt. Yang et al.[11] presented a new PdPt/CeO_2/C catalyst which shows excellent performance towards the anodic oxidation of formic acid. They believed that CeO_2 not only enhances the catalytic activity but also changes the mechanism of its catalysis of the anodic oxidation of formic acid exhibiting 60% higher activity than Pd/C. However, the origin for these interesting properties still remains obscure. Placing metal nanoparticles on ceria, not only increase metal dispersion but also promote catalytic redox properties by some kind of unspecified synergistic effect at the interface. More importantly, the nature of a particular type of ceria surface, linking with these phenomena and the underlying principles have not been carefully studied and optimized. There have sometimes been conflicting claims that metal-ceria rods with exposed (110)/(100) surfaces gave the best activity than other ceria morphologies[12] whereas metal-ceria cubes showed superior performances.[13] In general, ceria nanoparticles present the highest surface area and smallest crystalline size, leading to the most active of these structures. Ceria rods sample with higher surface area shows higher activity than that of ceria

cubes for the conditions that substrate gives weak adsorption strengths on their surfaces. However if the conditions chosen favor strong substrate adsorption especially when catalytic activity is normalized by unit surface area, the observed reactivity follows for rods based sample < cubes based sample which is directly related to the concentration of surface oxygen vacancies as a result of the exposure of the (1 1 0) and (1 0 0) preferential planes. Obviously, their surface area, nature of surface and depth of accessible oxygen of ceria which are highly dependent on reaction conditions, are the important factors. This present study is concerned with the studies of different ceria surfaces to host Pd nanoparticles for electro-oxidation of formic acid and correlation with catalytic activity and stability. The relationship between shape of ceria, concentration of oxygen vacancies, oxygen storage capacity, and oxygen mobility and the underlying mechanisms will be particularly investigated.

Synthesis of four different shapes of ceria nanoparticles namely: cubes, spheres, rods and plates were carefully carried out (S1.1 in SI). For example, the typical average particle size of ceria cubes with predominantly polar (100) surface of 21.5 ± 6.0 nm (BET surface area of 22 m^2 g^{-1}) and ceria rods of 6.5 ± 1.6 nm in width and 136 ± 23 nm in length with non-polar surface (110) (BET surface area of 75 m^2 g^{-1}) are shown in Figure 1 and Figure S1. There have been assignments for principle termination facets based on theoretical crystal structure and morphologies but surface disorders and reconstructions on these powder samples might have also taken place. For reliable correlation of surface structure-activity relationship, experimental determinations of the facets are required. Exit wave restoration of a focal series of HRTEM images simplifies the image by reducing residual abberations of the microscope and in Figures 1a,b show distinctive layers of cationic cerium (Ce^{4+}) and anionic oxygen layers in (100) terminal surface can be directly visualized and indexed. Such charge separation in alternative

layers can generate surface polarity. Whereas, the principal surface for rods ceria in Figures 1c,d are found to be (110) with inter-dispersed cerium cations and oxygen anions but mixed with small degrees of other reconstructed surfaces of (111) and (100). After Pd deposition, the morphologies of ceria were maintained (Figure S2). The size of Pd on rods and cubes were in range 3.4-3.5 nm which was close Pd colloid size (3.4 ± 0.7 nm) used.

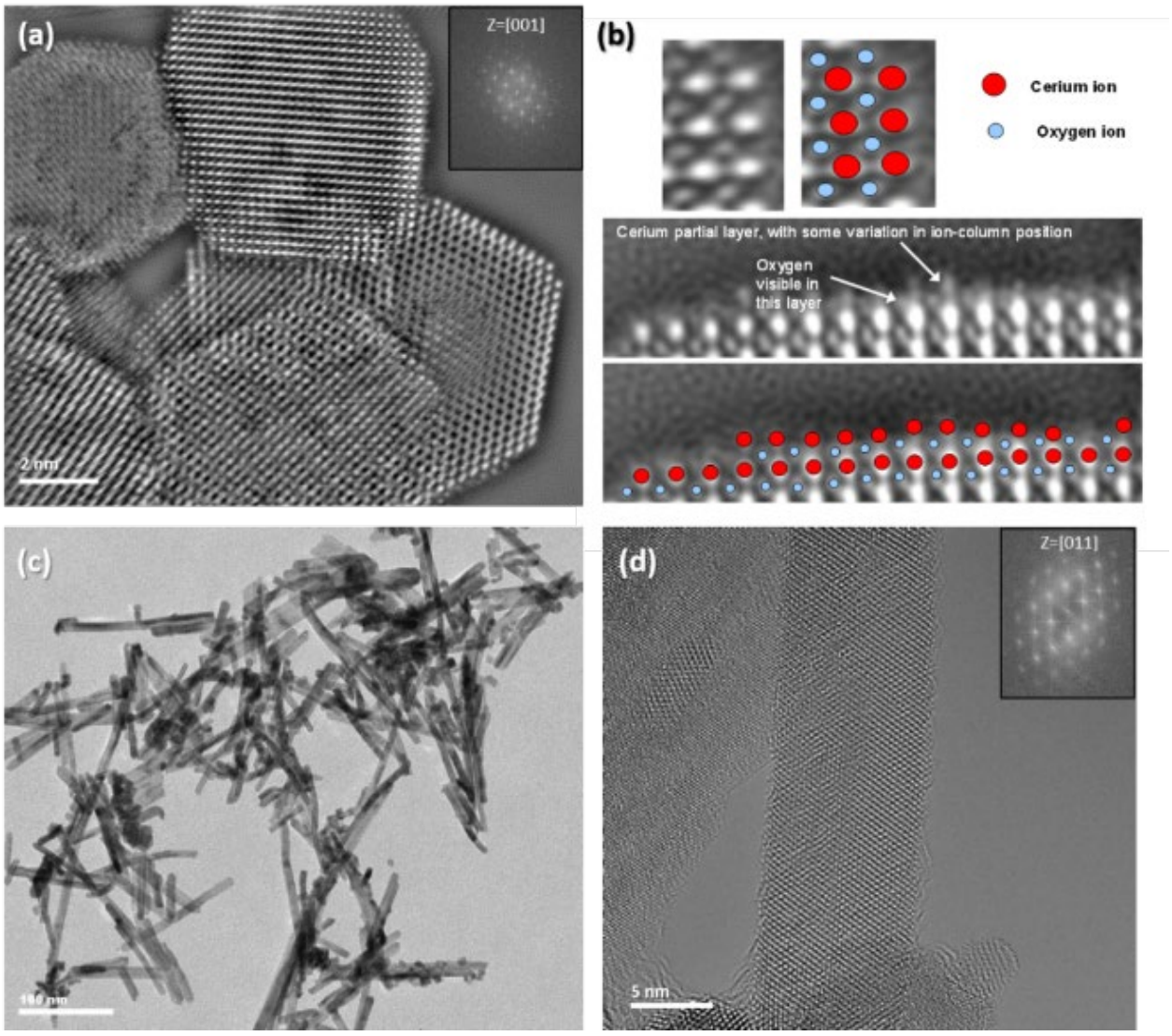

Figure 1. (a) Exit wave restoration image of ceria cubes with predominate polar (100) surfaces where deviations to hexagonal shape with reconstructed (111) facets can be seen; (b) High

magnification of the exit wave restoration showing the (100) showing discrete alternative atomic layers of $Ce^{3+/}Ce^{4+}$ and O^{2-} ions can be visualized and indexed matching with corresponding (100) model; (c) TEM image of rods ceria; (d) predominate polar (110) surface with inter-dispersed cerium cations and oxygen anions but also containing small degrees of other reconstructed surfaces of (111) and (100) surfaces.

Electro-catalytic activity and stability of the Pd deposited on different shaped ceria nanoparticles catalysts were evaluated by cyclic voltammetry (CV), CO stripping and chronoamperometry (CA) with the chosen conditions for extensive electrochemical reduction-oxidation. The steady state CV profile in 0.5 M H_2SO_4 is depicted in Figure 2a, which exhibits a typical hydrogen adsorption/desorption peak in the region of -0.2-0.1 V vs. Ag/AgCl. The oxide formation (OH_{ads}, O_{ads}) appears at about 0.6 V and the reduction of these species in range 0.25-0.45 V. Pd with or without blending with ceria rods show comparable activity but it is very interesting to note a significantly higher activity of cubes ceria giving higher mass activity (A/g-Pd) and specific activity (mA cm^{-2}) with taken Pd amount and surface area into account (Table S3). Cyclic voltammogram of formic acid electro-oxidation in 0.5 M H_2SO_4 is presented in Figure 2b. The anodic current reaches maxima at around 0.2V corresponding to formic acid oxidation through dehydrogenation pathway.[14] At higher potentials (> 0.2V), the oxidative current decreases because CO formed from stepwise formic acid oxidation adsorbs on Pd surface and blocks the active site of Pd.[14-15] Interestingly, Pd on cubes ceria, despite its lower BET surface area than rods, appears to be less susceptible to CO poisoning showing the highest electrochemical active surface (93 cm^2 g-Pd^{-1}) than other samples. This gives the cubes at least 2 times higher activity than rods of (110) surface, plates (surfactant poisoned (100) surface) and spheres ((111) surface) samples (Table S3). Figure 2c clearly shows that cubes ceria containing

(100) surface could indeed oxidise the CO adsorbed on Pd at the materials interface from typical CO stripping experiment at lower potential as compared with other ceria surfaces. It appears to be able to provide more active mobile oxygen species from beyond this ceria facet to remove the surface CO poison more readily. Similar results of the samples with and without activated carbon were obtained (SI). Chronoamperometry measurements show that the current density shown in Figure 2d rapidly decays to nearly zero value, indicative that surface of Pd nanoparticle is unable to oxidise CO or related species fast enough to avoid their poisoning at this potential. However, Pd on cubes ceria with polar (100) surface, yet again, shows both the initial and sustainable higher activity at steady current values that demonstrates a larger degree of accessible oxygen. This may suggest that this surface could extensive transfer active oxygen beyond the surface layers to oxidative remove CO or other related poisons more efficiently.

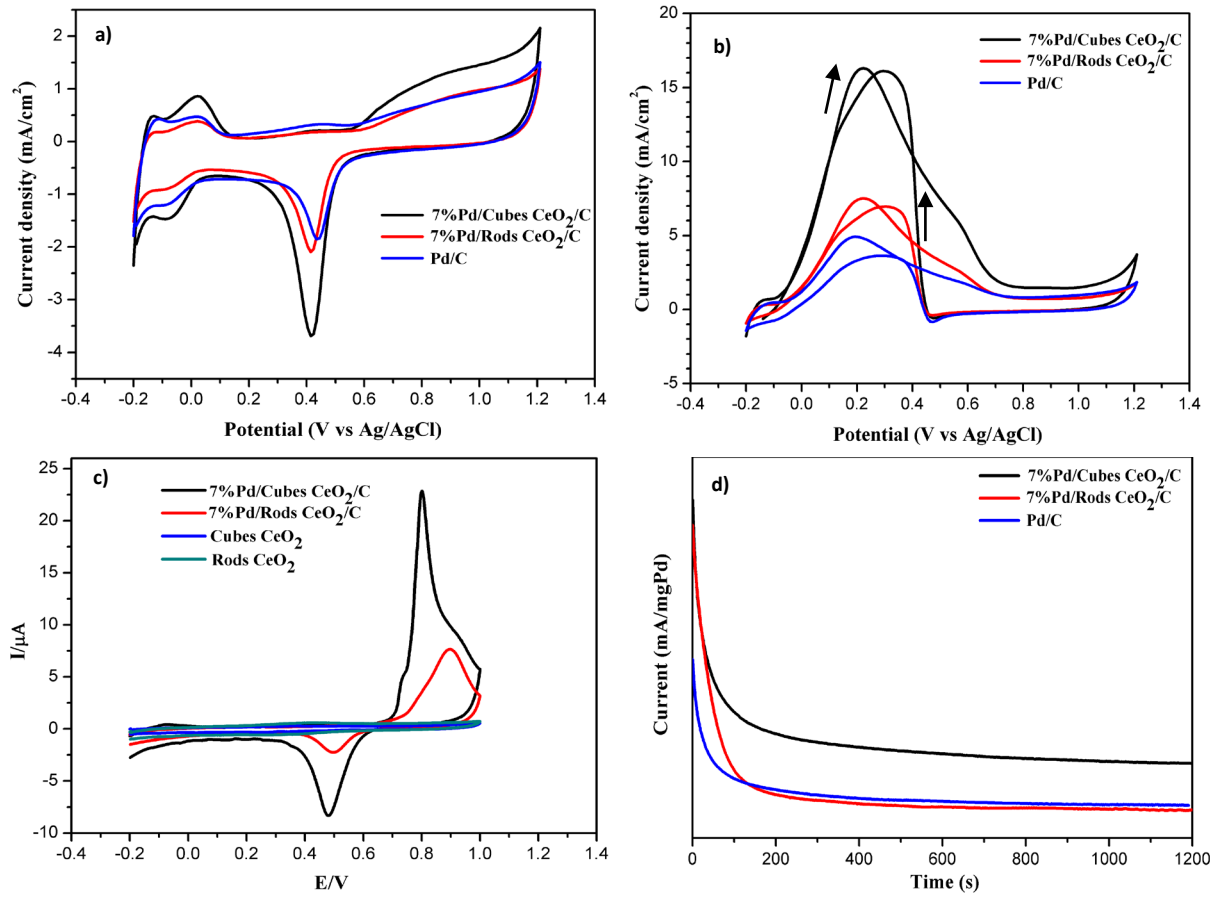

Figure 2. Electrocatalytic activity and stability studies of various Pd/ceria catalysts: (a) cyclic voltammetry in 0.5 M H_2SO_4 at scan rate 5 mV s^{-1}; (b) cyclic voltammetry in 0.5 M HCOOH and 0.5 M H_2SO_4 at scan rate 0.1 Vs^{-1} with arrows indicating the scanning direction; (c) CO stripping voltammograms; (d) chronoamperometry of HCOOH oxidation of different Pd/ceria catalysts compared to Pd/C with activated carbon in 0.5 M HCOOH and 0.5 M H_2SO_4 at potential 0.1 V.

It is interesting to note that the high intrinsic activity of cubes sample is apparently not correlated to the BET surface area or Pd dispersion but rather the nature of the polar (100) surface (sections S1 and S2). It is no doubt that the size of ceria can affect the catalytic performance. Previously, we reported that catalytic activity on ceria can strongly influenced by the size of ceria if the particle is at or below 5nm.[4] Such the quantum size dependent oxygen

storage capacity from O_2 adsorption on its surface was also clearly shown. However, for this present work, we used ceria nanoparticles with different facets which were larger than 5nm. We therefore attribute the superior catalytic activity to the dominant effect of a particular facet (shape), especially the higher energetic polar surface. As a result, relationship between shape of ceria nanoparticles, concentration of oxygen vacancies, and activity on formic acid electro-oxidation was investigated. The cubes ceria with or without Pd gave consistently an order of magnitude higher concentration of oxygen vacancies than rods with nonpolar (110) and spheres with (111) surface per gram basis (Table S2). The key questions are; why the polar (100) surface is more oxygen deficient than other ceria surfaces, and how can oxygen be transferred from this facet to Pd electrochemically to regenerate the metal surface so readily? During the evaluation of the Pd metal surface by CO chemisorption technique we have also encountered the interference from the surface mobile oxygen species of the polar (100) even in the presence of H_2 atmosphere. The large 'pseudo' deviation from Pd particle size (3.4 ± 0.7 nm) on cubes surface using CO chemisorption (such large Pd particle was actually not detected by XRD or TEM) after the H_2 pre-reduction shown in Table 1 clearly suggests the access of extensive mobile surface oxygens beyond this unique surface to reduce the CO chemisorption value on Pd until the {O} content in the polar ceria (100) layers are extensively reduced at above 400^{o}C (the calculation of Pd size was based on metal site: CO = 1:1).

Table 1. Particle sizes and surface areas of Pd derived from CO chemisorption; samples were calcined at different temperatures in H_2 for an hour before cooled to ambient temperature for CO chemisorption test.

Calcination Temp (ºC)	Particle size (nm)		Surface Area of metal (m^2/g)	
	Pd/CeO_2 (cubes)	Pd/CeO_2 (rods)	Pd/CeO_2 (cubes)	Pd/CeO_2 (rods)
100	30.1	3.2	16.60	153.91
200	16.8	3.3	29.65	151.44
300	7.2	2.9	72.42	152.30
400	4.6	3.3	109.01	155.13

In order to assess the dynamic redox properties of the polar (100) surface versus non-polar (110) on overlying Pd nanoparticle, surface composition of Ce^{4+}/Ce^{3+} and Pd^{2+}/Pd^0 was carefully characterised using ambient pressure (AP) XPS, where measurements were performed by switching the sample feed to reducing or oxidising gases in operando.[16] Without a strong support oxide to buffer the redox properties of the overlying noble metal nanoparticle, it was anticipated that the metal should quickly switch to a metal oxide form or vice versa upon changing gas composition. To investigate this firstly, a Pd on rods ceria sample was heated in 1 torr H_2 gas to 500 °C to fully reduce the Pd surface which catalysed further reduction to nearby ceria surface. This sample was then cooled to 100 °C under H_2 before conducting XPS measurement. Similarly, the sample was then re-oxidised in 1 torr O_2 gas at 300 °C before cooling to 100 °C in

O_2 for the XPS measurement. The six peaks resulting from spin orbit-splitting of 3d core level and additional peaks due to 'shake-down' states where electrons are transferred from the O 2p level to the Ce 4f level in the excited state together with Pd^{2+}/Pd^0 peaks can be found in section S4. As seen from Figure 3a, the summarized data suggest that Pd^{2+} has been reduced to give higher content of Pd^0 with corresponding rise in surface Ce^{3+}/Ce^{4+} ratio to 0.3 ± 0.05 (Figure 3b) in H_2. Calibration (S4) indicated that this value corresponds to the boundary phase of Ce_2O_3 on the top surface. Upon re-oxidation, nearly reversible changes in Ce^{3+}/Ce^{4+} composition on rods with non-polar (110) surface without accessing much to oxygen species for buffering these changes can also be seen. On a contrary, the data in Figure 3c suggest that the ceria cubes sample with (100) surface gives a lower Pd^{2+}/Pd^0 peak ratio under vacuum at the beginning, upon reduction, and re-oxidation. It is surprising to find a resistance in converting Pd^{2+} to Pd^0 during the reduction stage, which can be explained by the oxygen being transferred or buffered from the metal-ceria surface to the metal. Similarly, resistance for the conversion of Pd^0 to Pd^{2+} is also encountered despite the fact that the surface re-oxidation on Pd^0 should have been readily taken place under oxidation conditions (mobile oxygen is continuously removed from Pd surface to ceria cubic surface as opposite to reversed observation in CO chemisorption experiment). It is noted that the maintenance of the $Ce^{3+/}Ce^{4+}$ ratio, around 0.3 (Ce_2O_3), around the top surface of the previously reduced state in Figure 3d despite being in an O_2 atmosphere implies that the re-oxidation of Ce^{3+} to Ce^{4+} catalysed by Pd is not yet completed from the extensively reduced inner layers created from the previous reduction treatment. This result echoes the reported surface properties of ceria with high oxygen storage capacity of (100) ceria surface and high mobility of oxygens at noble metal-ceria interface to resist to the change in metal oxidation state.[17] This means a significant amount of O species on Pd is rapidly spilling and replenishing

the oxygen vacancies to ceria nanoparticle via this ceria cubes (100) surface during the dynamic re-oxidation process to maintain the higher content of Pd^0. It is interesting to note that by using STEM-EELS mapping Turner et al.[18] have recently demonstrated that (100) ceria can also provide more oxygen beyond the top layer for more extensive surface reduction than that of (111) surface.

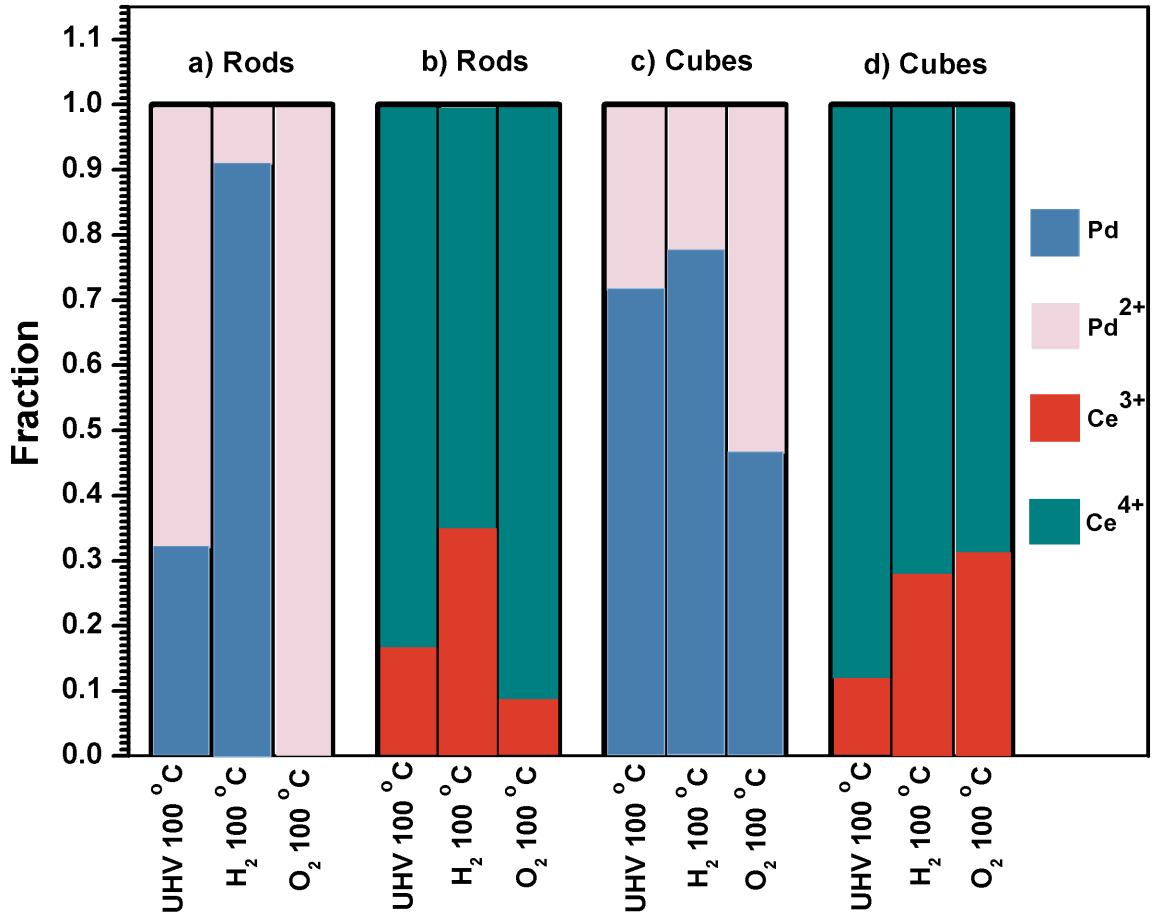

Figure 3. The changes in surface composition derived from AP-XPS (a) Pd^{2+}/Pd^0 in 7% Pd/ceria rods; (b) Ce^{3+}/Ce^{4+} in 7% Pd/ceria rods; (c) Pd^{2+}/Pd^0 in 7% Pd/ceria cubes; (d) Ce^{3+}/Ce^{4+} in 7% Pd/ceria cubes upon switching from UHV (UHV 100 °C) to reducing gas (H_2 100 °C) and oxidising gas (O_2 100 °C) conditions.

It is noted that the negative end of polar (100) ceria surface has been reported by Kim et. al. which is terminated by O in their direct recoil spectroscopy/low energy ion scattering of Kr experiments.[19] As stated, a strong net dipole moment perpendicular to the surface due to alternately charged planes with a repeating unit consisting of only two planes which is termed a polar surface.[20] Here, we have confirmed such atomic arrangement in ceria cubes (100) surface (Figure 1). The strong electrostatic repulsion of the same charge ions on the same planes means that this is a high energy unstable surface. There are ways to reduce the unstable surface polarity such as adsorption of counter-ions or generating oxygen vacancies by altering the oxidation state of metal ions.[21] The calculated energies for oxygen vacancy formation from polar (100) and non-polar (110) and (111) ceria surfaces according to our DFT models (see Section S5 of SI) have been carried out. Figure S10 shows the structural models of (111), (110) and (100) ceria surfaces. The (100) surface has been reported by Kim et al. to be terminated by O in their direct recoil spectroscopy / low energy ion scattering of Kr experiments.[19] It also has been argued to produce a net dipole moment perpendicular to the surface due to alternately charged planes with a repeat unit consisting of only two planes which is termed a polar surface.[20] The calculated surface energy of ceria shown in Table 2 indicates that stability is in the order (111) < (110) < (100). On the other hand, upon reconstruction of (100) to remove the dipole moment ($100_{\text{O-half}}$), the stability of (100) and (110) are reversed as suggested by the less favorable oxygen vacancy formation (2.40 and 1.99 eV, respectively). Furthermore, when one oxygen atom is added into the reconstructed (100) surface ($100_{\text{O-half + 1}}$), the oxygen vacancy formation becomes very favorable. This suggests that between the unconstructed (100) surface and one oxygen added to the reconstructed surface, the oxygen vacancy formation is more favorable than the (110) surface, implying (100) is the less stable surface in the surface CeO_x, $1 < x \leq 2$ range.

Table 2. DFT calculated energy of oxygen vacancy formation of ceria surfaces.

Surface	Calculated energy of oxygen vacancy formation (eV)
111	3.08
110	1.99
100	-1.98
$100_{\text{O-half}}$	2.40
$100_{\text{O-half + 1}}$	-1.56

The observations on the catalyst testing demonstrate that the ceria cubes support with polar surface is more superior to the rods and other shapes, in terms of oxygen mobility and oxygen vacancy formation. It could be postulated that these characteristics are attributed to the polarity of (100) surface, at which under reaction conditions, being at the state of more than half filled oxygen CeO_x ($1 < x \leq 2$), which gives them the higher degree of oxygen vacancy formation and oxygen mobility during catalysis. At this state, the ceria (100) surface has a non-zero dipole moment perpendicular to surface, therefore a polar surface which could possibly contribute to its surface properties through electrostatic interactions.

Noticeably, -1.98 eV is obtained in the polar (100) indicating that a spontaneous formation of oxygen vacancies until half of oxygen atoms are removed (no further polarity) versus the positive values for other non-polar surfaces. This can explain our observation of higher concentration of oxygen vacancies we measured via this surface. Furthermore, when one oxygen atom is added into the reconstructed (100) surface (O-half +1) in our model, the oxygen vacancy formation suddenly returns to be extremely favourable due to the strong electrostatic repulsion (-1.56 eV). In addition, high energy for oxygen vacancy formation is anticipated when oxygen is

below the half stoichiometry with no polarity. This clearly suggests that the tendency for oxygen mobility to and from Pd may depend on the polarity of (100) with such alternative charge arrangements in progressive layers. With reference to Scheme 1, we have found that under dynamic short time exposure of oxidising species such as O_2 of Pd (as like a pulse) whereby the metal can respond more quickly, the deficient oxygen from half-stoichiometry of ceria (100) in steady reducing environment can capture the oxygen from Pd surface. Whereas re-oxidation of Pd (for removal of CO pulse) can also be taken place by the oxygen surplus (100) surface layers in oxidising environment (under positive potential), giving rise to fast redox properties and oxygen storage capacity due to the facile change in oxidation state of cerium ions and the availability of oxygen sites for these surface layers. We argue that such oxygen storage and mobility phenomena at metal-ceria (100) interface are thus not related to natural oxygen diffusion process on surface but associated with the thermodynamic stability of the (100) surface ionic arrangements. This can provide unique surface redox properties to account for the high activity and stability observed in electro-oxidation of formic acid. In addition, the morphology of the support in some cases could also further stabilize the adsorbed species by directly interacting with the support or indirectly through metal-support interaction and make their removal faster.. There have been some DFT calculations in the literature on this point. For example, Nolan and Watson [22] presented the structure and energetics of CO adsorbed onto stoichiometric and reduced (111), (110), and (100) surfaces of ceria from first principles density functional theory corrected for on-site Coulomb interactions, DFT+U. They reported that the interaction is strongly surface dependent. Upon interaction of CO with the (111) surface, weak binding is found with an adsorption energy of -6 kcal/mol. For the (110) and (100) surfaces, interaction with CO leads to formation of a surface $(CO_3)^{2-}$ species, in which two oxygen atoms are pulled out of the surface.

The interaction has an adsorption energy of -45 kcal mol^{-1} (110) and -74 kcal mol^{-1} (100), supporting that the additional stabilization of the CO adsorption on (100) facet could make the CO removal faster. It is noted that the thermodynamic obtained from our DFT calculations shows that the energy preference toward the easier formation of vacancies in cubic shape ceria. However, kinetic factors might hinder the diffusion process. A kinetic study of oxygen diffusion path over the Pd on nanocubic (100) in comparison with other ceria facets may provide the support basis for the observed higher electrocatalytic activity. On the contrary, the kinetic pathway is highly dependent on grain boundaries in powder sample and if for defined crystal surface, the actual surface feature and defect concentration of the particular facet. It is unfortunate that the surface structure of ceria is not static, and the inherent mobility of atoms at ceria surfaces must be assessed for a better understanding of the temporal evolution of the atomic structure of facets. The main challenges in deriving the surface feature of a particular CeO_2 facet in the HRTEM is its notorious ability to reduce easily under irradiation from the electron beam and is also critically dependent vacuum/atmosphere used. Without acquiring the surface features of CeO_2 facets it may be difficult to address the kinetic pathway/activation step from both experimental and modelling approaches. It is noted that Epicier and co-workers [23] have recently reported the variation of surface features due to high mobility at {100} surfaces of ceria in the environmental transmission electron microscope. Further experimental and theoretical works are therefore required to investigate the dynamic oxygen mobility of the (100) facet and its high electrocatalytic activity.

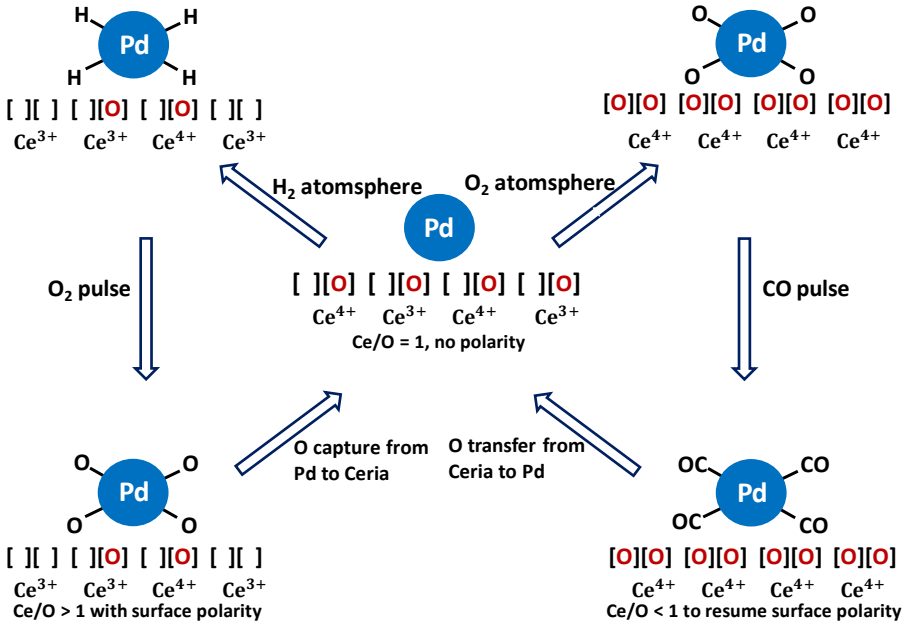

Scheme 1. Pd metal on CeO_2 can gain access to mobile oxygen atoms of (100) surface and beyond reversibly through the alternative cations and anions layers arrangement due to change in polarity with the same planes (Pd exerts a greater sensitivity to changing gas environment over ceria).

In conclusion, we have identified cubic shape provides much larger access of mobile oxygen atoms reversibly via (100) polar surface to overlying noble metal nanoparticles than that of rod shape particle containing mainly (110) facets, which could assist removal of strongly adsorbed poison species on metal surface to sustain higher electrocatalytic activity. This surface with alternative layers of oxygen ions and cerium ions by STEM image with exit wave restoration is confirmed. The strong tendency of the (100) ceria to reduce polarity according to our DFT calculation could allow the overlying noble metal to gain greater access to the active mobile

oxygen atoms beyond the top surface from this support with controlled morphology. As a result, for conditions involving deep reduction and oxidation during catalytic cycle, more superior performance of metal-ceria cubes interface than other morphologies can be resulted despite the lower surface area of cubes used.

AUTHOR INFORMATION

Corresponding Author

Franklin Tao (franklin.feng.tao@ku.edu); Karaked Tedsree (karaked@go.buu.ac.th) and Edman Tsang (edman.tsang@chem.ox.ac.uk)

Present Addresses

(1) The Department of Chemistry, Fudan University, Shanghai, China for LY (yelin@fudan.edu.cn)

(2) Centre for Advanced Materials and Energy Sciences (CAMES), Universiti Brunei Darussalam, Brunei for AHM (hanif.mahadi@ubd.edu.bn)

(3) Department of Chemistry, Faculty of Science, Burapha University, Bangsaen, Chonburi, 20131 Thailand for CS (nam_scim@hotmail.com) and KT (karaked@go.buu.ac.th)

(4) SINOPEC, Beijing for JQ (qujin1797@gmail.com)

(5) College of Materials Science and Engineering, Fuzhou University Town, Fuzhou, 350108 P. R. China for XF (xufeng.mater@fzu.edu.cn)

(6) School of Materials, University of Manchester, Manchester M13 9PL UK for SMF (simon.fairclough@manchester.ac.uk).

(7) Department of Materials, University of Oxford, Oxford OX1 3PH, UK for NPY (neil.young@materials.ox.ac.uk)

(8) Department of Chemistry, University of Kansas 1501 Wakarusa Dr. Lawrence, KS 66047, USA for JS (junjun.shan.5@gmail.com), LN (luan.nguyen.nd@ku.edu) and FFT (franklin.feng.tao@ku.edu)

(8) Wolfson Catalysis Centre, Department of Chemistry, University of Oxford, Oxford, OX1 3QR, UK for PH (ping-luen.ho@univ.ox.ac.uk) and SCET (edman.tsang@chem.ox.ac.uk)

Author Contributions

‡Lin Ye and Hanif Mahadi contributed equally.

Funding Sources

The support of this project from the EPSRC of UK (EP/K040375/1) to Oxford is gratefully acknowledged.

Notes

The authors declare no competing financial interests.

Supporting Information

Detailed preparation procedures, testing, material characterization and DFT calculation. The Supporting Information is available free of charge on the ACS Publications website.

ACKNOWLEDGEMENT

The authors wish to thank Diamond Light Source and SUPERSTEM of Darebsury UK for the access of high resolution aberration corrected TEM and STEM, respectively.

REFERENCES

1. (a) Trovarelli, A., Catalytic Properties of Ceria and CeO_2-Containing Materials. *Catalysis Reviews* **1996,** *38*, 439-520; (b) Zhou, K.; Wang, X.; Sun, X.; Peng, Q.; Li, Y., Enhanced

catalytic activity of ceria nanorods from well-defined reactive crystal planes. *Journal of Catalysis* **2005,** *229*, 206-212; (c) Han, W.-Q.; Wen, W.; Hanson, J. C.; Teng, X.; Marinkovic, N.; Rodriguez, J. A., One-Dimensional Ceria as Catalyst for the Low-Temperature Water−Gas Shift Reaction. *The Journal of Physical Chemistry C* **2009,** *113*, 21949-21955.

2. Trovarelli, A., Structural and Oxygen Storage/Release Properties of CeO_2-Based Solid Solutions. *Comments on Inorganic Chemistry* **1999,** *20*, 263-284.

3. Trovarelli, A.; Llorca, J., Ceria Catalysts at Nanoscale: How Do Crystal Shapes Shape Catalysis? *ACS Catalysis* **2017,** *7*, 4716-4735.

4. Xu, J.; Harmer, J.; Li, G.; Chapman, T.; Collier, P.; Longworth, S.; Tsang, S. C., Size dependent oxygen buffering capacity of ceria nanocrystals. *Chemical Communications* **2010,** *46*, 1887-1889.

5. Mai, H.-X.; Sun, L.-D.; Zhang, Y.-W.; Si, R.; Feng, W.; Zhang, H.-P.; Liu, H.-C.; Yan, C.-H., Shape-Selective Synthesis and Oxygen Storage Behavior of Ceria Nanopolyhedra, Nanorods, and Nanocubes. *The Journal of Physical Chemistry B* **2005,** *109*, 24380-24385.

6. (a) Acerbi, N.; Tsang, S. C. E.; Jones, G.; Golunski, S.; Collier, P., Rationalization of Interactions in Precious Metal/Ceria Catalysts Using the d-Band Center Model. *Angewandte Chemie International Edition* **2013,** *52*, 7737-7741; (b) Du, X.; Zhang, D.; Shi, L.; Gao, R.; Zhang, J., Morphology Dependence of Catalytic Properties of Ni/CeO_2 Nanostructures for Carbon Dioxide Reforming of Methane. *The Journal of Physical Chemistry C* **2012,** *116*, 10009-10016; (c) Sun, C.; Li, H.; Chen, L., Nanostructured ceria-based materials: synthesis, properties, and applications. *Energy & Environmental Science* **2012,** *5*, 8475-8505.

7. Yadav, M.; Xu, Q., Liquid-phase chemical hydrogen storage materials. *Energy & Environmental Science* **2012,** *5*, 9698-9725.

8. Tedsree, K.; Li, T.; Jones, S.; Chan, C. W.; Yu, K. M.; Bagot, P. A.; Marquis, E. A.; Smith, G. D.; Tsang, S. C., Hydrogen production from formic acid decomposition at room temperature using a Ag-Pd core-shell nanocatalyst. *Nature nanotechnology* **2011,** *6*, 302-7.

9. Wang, Y.; Wang, S.; Wang, X., CeO_2 Promoted Electro-Oxidation of Formic Acid on Pd/C Nano-Electrocatalysts. *Electrochemical and Solid-State Letters* **2009,** *12*, B73-B76.

10. Gu, D.-M.; Chu, Y.-Y.; Wang, Z.-B.; Jiang, Z.-Z.; Yin, G.-P.; Liu, Y., Methanol oxidation on Pt/CeO_2–C electrocatalyst prepared by microwave-assisted ethylene glycol process. *Applied Catalysis B: Environmental* **2011,** *102*, 9-18.

11. Yang, L.; Su, H.; Shu, T.; Liao, S., Enhanced electro-oxidation of formic acid by a PdPt bimetallic catalyst on a CeO_2-modified carbon support. *Science China Chemistry* **2012,** *55*, 391-397.

12. Ouyang, B.; Tan, W.; Liu, B., Morphology effect of nanostructure ceria on the Cu/CeO_2 catalysts for synthesis of methanol from CO_2 hydrogenation. *Catalysis Communications* **2017,** *95*, 36-39.

13. Tan, H.; Wang, J.; Yu, S.; Zhou, K., Support Morphology-Dependent Catalytic Activity of Pd/CeO_2 for Formaldehyde Oxidation. *Environmental Science & Technology* **2015,** *49*, 8675-8682.

14. Wang, X.; Hu, J.-M.; Hsing, I. M., Electrochemical investigation of formic acid electro-oxidation and its crossover through a Nafion® membrane. *Journal of Electroanalytical Chemistry* **2004,** *562*, 73-80.

15. Cuesta, A.; Cabello, G.; Osawa, M.; Gutiérrez, C., Mechanism of the Electrocatalytic Oxidation of Formic Acid on Metals. *ACS Catalysis* **2012,** *2*, 728-738.

16. Tao, F., Design of an in-house ambient pressure AP-XPS using a bench-top X-ray source and the surface chemistry of ceria under reaction conditions. *Chemical Communications* **2012,** *48*, 3812-3814.

17. Li, P.; Chen, X.; Li, Y.; Schwank, J. W., A review on oxygen storage capacity of CeO_2-based materials. *Catalysis Today* **2018**. in press. DOI: 10.1016/j.cattod.2018.05.059

18. Turner, S.; Lazar, S.; Freitag, B.; Egoavil, R.; Verbeeck, J.; Put, S.; Strauven, Y.; Van Tendeloo, G., High resolution mapping of surface reduction in ceria nanoparticles. *Nanoscale* **2011,** *3*, 3385-90.

19. Kim, Y. J.; Gao, Y.; Herman, G. S.; Thevuthasan, S.; Jiang, W.; McCready, D. E.; Chambers, S. A., Growth and structure of epitaxial CeO_2 by oxygen-plasma-assisted molecular beam epitaxy. *Journal of Vacuum Science & Technology A* **1999,** *17*, 926-935.

20. (a) Sayle, D. C.; Maicaneanu, S. A.; Watson, G. W., Atomistic Models for CeO_2(111), (110), and (100) Nanoparticles, Supported on Yttrium-Stabilized Zirconia. *Journal of the American Chemical Society* **2002,** *124*, 11429-11439; (b) Skorodumova, N. V.; Baudin, M.; Hermansson, K., Surface properties of CeO_2 from first principles. *Physical Review B - Condensed Matter and Materials Physics* **2004,** *69*, 075401; (c) Baudin, M.; Wójcik, M.;

Hermansson, K., Dynamics, structure and energetics of the (111), (011) and (001) surfaces of ceria. *Surface Science* **2000,** *468*, 51-61.

21. (a) Noguera, C.; Goniakowski, J., Polarity in Oxide Nano-objects. *Chemical Reviews* **2013,** *113*, 4073-4105; (b) Liu, X.; Zhou, K.; Wang, L.; Wang, B.; Li, Y., Oxygen Vacancy Clusters Promoting Reducibility and Activity of Ceria Nanorods. *Journal of the American Chemical Society* **2009,** *131*, 3140-3141.

22. Nolan, M.; Watson, G. W., The Surface Dependence of CO Adsorption on Ceria. *J. Phys. Chem. B* **2006**, 110, 16600-16606.

23. Bugnet, M.; Overbury, S. H.; Wu, Z. L.; Epicier, T., Direct Visualization and Control of Atomic Mobility at {100} Surfaces of Ceria in the Environmental Transmission Electron Microscope. *Nano Lett.* **2017**, 17, 7652-7658.